Ultrasound in Med. & Biol. Vol. 17, No. 2, pp. 187–194, 1991
Printed in the U.S.A.

0301-5629/91 $3.00 + .00

●*Original Contribution*

STATISTICAL UNCERTAINTY IN ULTRASONIC BACKSCATTER AND ATTENUATION COEFFICIENTS DETERMINED WITH A REFERENCE PHANTOM

LIN XIN YAO, JAMES A. ZAGZEBSKI and ERNEST L. MADSEN
Department of Medical Physics, University of Wisconsin, 1530 Medical Science Center, 1300 University Avenue, Madison, WI 53706, USA

(*Received* 7 *June* 1990; *in final form* 20 *August* 1990)

Abstract—Uncertainties in measured attenuation and backscatter coefficients due to statistical fluctuations in echo signal data from a randomly scattering medium are estimated. The uncertainties are computed for the special case in which a reference phantom is employed to account for transducer and instrumentation factors when measuring attenuation and backscatter coefficients. The resultant uncertainty in the attenuation is inversely proportional to the $\frac{3}{2}$ power of the depth range. The error in the backscatter coefficient arises both from the local fluctuation in the data and from the uncertainty in the attenuation estimate. The first of these is inversely proportional to the square root of the number of independent data points, while the second results in a contribution that is depth dependent. Predicted errors were tested by scanning tissue mimicking phantoms and estimating attenuation and backscatter coefficients for subsets of the digitized echo data. Standard deviations of the experimental results were in agreement with those predicted.

Key Words: **Attenuation coefficient, Backscatter coefficient, Statistical uncertainty, Reference phantom.**

INTRODUCTION

In a previous paper (Yao et al. 1990a) we described a relative processing method for determining the ultrasonic attenuation and backscatter coefficients of a medium. This method involves comparing frequency and depth-dependent echo data from the sample with corresponding data from a reference phantom, both data sets being recorded with the same transducer assembly, receiver gain, etc. The acoustic properties of the sample are derived from ratios of signals from the two media, along with the knowledge of the properties of the reference phantom.

This paper is concerned with uncertainties in backscatter coefficient and attenuation coefficient estimates using the reference phantom method. There are two categories of uncertainties present. One is methodological and instrumental, due, for example, to instrumental inaccuracy, presence of reverberations, effects of overlying tissue, nonuniformities in the medium and electronic noise. The second is statistical due to the random processes involved in forming the echo signal. It is these latter uncertainties that are the subject of this paper.

The purpose of the work reported here is to determine the magnitude of errors in measurements of backscatter coefficients and attenuation coefficients arising from statistical fluctuations in echo data when a medium containing a large number of randomly distributed scatterers is investigated. The echo signal from such a medium is the outcome of a random process. Previous investigators have estimated uncertainties in the attenuation coefficient under these conditions (Kuc 1985; Parker 1986; He and Greenleaf 1986; Ophir et al. 1985), but the results on backscatter have not been treated. Error propagation, starting with uncertainties due to statistical fluctuations in echo signal data, is used to compute resultant uncertainties in attenuation coefficients and then in backscatter coefficients. These uncertainties involve the number of independent data samples used in the estimation, the overlying attenuation and the depth interval from which echo signals are recorded. Examples are given comparing expected standard deviations with actual results from experimentally recorded data.

REFERENCE PHANTOM METHOD

The data acquisition method is illustrated in Fig. 1. A pulse-echo transducer transmits an ultrasound

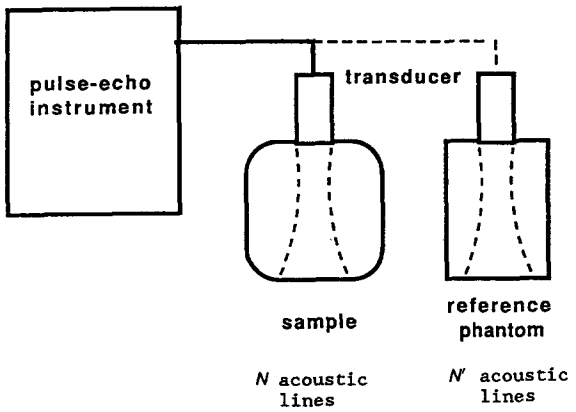

Fig. 1. The data acquisition of the reference phantom method. The radio-frequency echo signal is acquired from the region of interest in the sample; the signal is also obtained from the reference phantom using the same instrumentation and control settings.

beam into the sample which contains Rayleigh or intermediate sized scatterers. The echo signal voltage, $v(t)$ is recorded as a function of time, t. $v(t)$ is bandpass filtered at frequency ω_1, and the square of the amplitude of the filtered signal, $i(\omega_1, t)$, is detected. This sequence is repeated for different locations of the transducer, yielding a number of $i(\omega_1, t)$'s; these are used to calculate a mean square echo signal, $I(\omega_1, t)$ for the sample. The same procedure and same scanner settings are then used to obtain corresponding data, $I'(\omega_1, t)$ from the reference phantom.

Let $BSC(\omega_1)$ and $\alpha(\omega_1)$ be the backscatter coefficient and attenuation coefficient at angular frequency ω_1 of the sample, and $BSC'(\omega_1)$ and $\alpha'(\omega_1)$ the corresponding values for the reference phantom. When a narrow band filter is used, the analysis by Yao et al. (1990a) leads to

$$\frac{I(\omega_1, t)}{I'(\omega_1, t)} = \frac{I(\omega_1, z)}{I'(\omega_1, z)} = \frac{BSC(\omega_1)e^{-4\alpha(\omega_1)z}}{BSC'(\omega_1)e^{-4\alpha'(\omega_1)z}} \quad (1)$$

where signals occurring at time t are assumed to have originated from the depth $z = ct/2$, c being the speed of sound in the medium. We have assumed that the sample and the reference phantom have uniform properties throughout their volumes.

Let $RI(\omega_1, z)$ be the ratio of the average squared-amplitude from the sample to that from the reference phantom corresponding to depth z. Also, let $RB(\omega_1)$ be the ratio of the backscatter coefficient of the sample to that of the reference phantom, and $\Delta\alpha(\omega_1) \equiv \alpha(\omega_1) - \alpha'(\omega_1)$, be the difference between the attenuation coefficients of the two media. Equation (1) then becomes

$$RI(\omega_1, z) = RB(\omega_1)e^{-4\Delta\alpha(\omega_1)z}. \quad (2)$$

Define

$$X(\omega_1, z) \equiv \ln[RI(\omega_1, z)]. \quad (3)$$

Taking logarithms of both sides of eqn (2), we have

$$X(\omega_1, z) = \ln[RB(\omega_1)] - 4\Delta\alpha(\omega_1)z. \quad (4)$$

A least squares analysis is used to fit the function $X(\omega_1, z)$ vs. depth to a straight line, *i.e.*, $X = a + bz$. The slope of this line yields the difference between the attenuation coefficients of the sample and the reference phantom. Once $\Delta\alpha(\omega_1)$ is known, the backscatter coefficient ratio can be determined using eqn (2). The backscatter and attenuation coefficients are known for the reference phantom; thus, the analysis yields values for the sample.

UNCERTAINTY PROPAGATION

Error analysis will be done for measuring backscatter and attenuation coefficients of a macroscopically uniform materal assumed to have a large number of randomly distributed scatterers. Thus, the squared-amplitude, $i(\omega_1, z)$ is a random variable. Its expected value is $\langle i(\omega_1, z)\rangle$ and its standard deviation is $\sigma_i(\omega_1, z)$. The signal-to-noise ratio of the squared-amplitude, SNR_0, is

$$SNR_0 = \langle i(\omega_1, z)\rangle / \sigma_i(\omega_1, z). \quad (5)$$

For cases where Rayleigh statistics (Wagner et al. 1983) apply, SNR_0 is 1, and this simplifies the analysis somewhat. However, echo signals from soft tissues do not necessarily follow Rayleigh statistics (Tuthill et al. 1988). Consequently, this restriction is not imposed in the following derivations.

Attenuation coefficient

The standard deviation of $I(\omega_1, z)$ is $\sigma_I(\omega_1, z)$. If $I(\omega_1, z)$ is a result of averaging N independent measurements of the squared echo amplitude, $i(\omega_1, z)$, then

$$\sigma_I(\omega_1, z) = \frac{\sigma_i(\omega_1, z)}{\sqrt{N}} = \frac{k}{\sqrt{N}}\langle i(\omega_1, z)\rangle \quad (6)$$

where $k \equiv 1/SNR_0$. If we use the average squared-amplitude, $I(\omega_1, z)$, which is equal to $\overline{i(\omega_1, z)}$, as an estimate of the expectation value of the squared-amplitude, $\langle i(\omega_1, z)\rangle$, eqn (6) becomes

$$\sigma_I(\omega_1, z) = \frac{k}{\sqrt{N}} I(\omega_1, z). \quad (7)$$

Similarly, for the reference phantom

$$\sigma_{I'}(\omega_1, z) = \frac{k}{\sqrt{N'}} I'(\omega_1, z) \tag{8}$$

where N' is the number of independent measurements involved, and we have assumed the same signal-to-noise ratio for the reference phantom and the sample. The analysis may easily be generalized to the situation where the SNR_0's are not identical.

$I(\omega_1, z)$ and $I'(\omega_1, z)$ in eqn (1) are obtained from two media and are statistically independent. The standard deviation of their ratio, $RI(\omega_1, z)$, denoted by $\sigma_{RI}(\omega_1, z)$, satisfies

$$\frac{\sigma_{RI}^2}{RI^2} = \frac{\sigma_I^2}{I^2} + \frac{\sigma_{I'}^2}{I'^2} = \frac{k^2}{N} + \frac{k^2}{N'} = \frac{N + N'}{NN'} k^2. \tag{9}$$

Referring to eqn (3), the standard deviation of $X(\omega_1, z)$ is given by

$$\sigma_X = \frac{\partial X}{\partial RI} \sigma_{RI} = \frac{\sigma_{RI}}{RI}, \tag{10}$$

or from eqn (9)

$$\sigma_X = k \sqrt{\frac{N + N'}{NN'}}. \tag{11}$$

The slope of the linear fit of $X(\omega_1, z)$ vs. z is calculated using data points corresponding to a depth interval whose length is Z (see Fig. 2). The standard deviation of the slope, $\sigma_b(\omega_1, z)$, due to uncertainties in $X(\omega_1, z)$ is given by (Bevington 1969)

$$\sigma_b = \frac{\sigma_X}{\sqrt{n}\sqrt{(z - z_0)^2}} \tag{12}$$

where n is the number of measurements of $X(\omega_1, z)$ in the interval Z such that the values obtained are not correlated, *i.e.*, they are statistically independent; z refers to the coordinate of individual data points; z_0 is the depth of the center of the segment and the bar is an average operation. The mean square magnitude, $\overline{(z - z_0)^2}$, can be estimated using

$$\overline{(z - z_0)^2} \approx \frac{1}{Z} \int_{z_0 - Z/2}^{z_0 + Z/2} (z - z_0)^2 \, dz = \frac{Z^2}{12}. \tag{13}$$

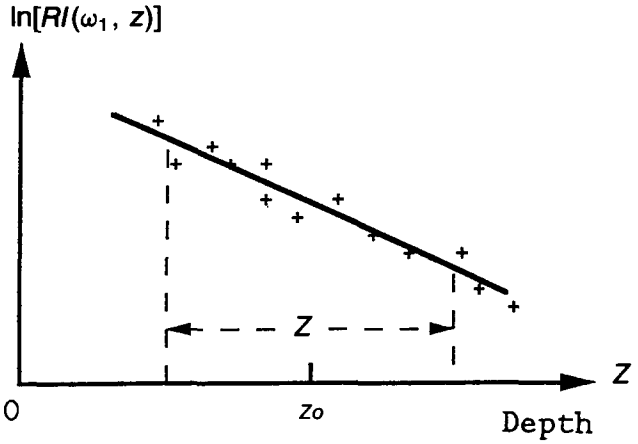

Fig. 2. Typical plot of $X(\omega_1, z)$, the logarithm of the ratio of the echo squared-amplitude from the sample to that from the reference phantom, vs. depth. The region of interest (ROI) is from z_1 to z_2; the midpoint of the ROI is at depth z_0, and the length of the depth interval is Z, which is equal to $z_2 - z_1$.

Thus,

$$\sigma_b = \frac{\sqrt{12}\sigma_X}{\sqrt{n}Z}. \tag{14}$$

From eqn (4), we have $\Delta\alpha(\omega) = b/4$; the standard deviation of $\Delta\alpha(\omega_1)$ is $\frac{1}{4}$ that of b. Since $\alpha'(\omega_1)$ is known, the standard deviation of $\alpha(\omega_1)$, $\sigma_\alpha(\omega_1)$, resulting from statistical fluctuations is

$$\sigma_\alpha = \frac{\sqrt{3}\sigma_X}{2\sqrt{n}Z} = \frac{k\sqrt{3}\sqrt{N + N'}}{2\sqrt{n}Z\sqrt{NN'}} \text{ (nepers/cm)}, \tag{15}$$

or using the more familiar unit dB/cm

$$\sigma_\alpha = \frac{7.52k\sqrt{N + N'}}{\sqrt{n}Z\sqrt{NN'}} \text{ (dB/cm)}. \tag{16}$$

Thus, the uncertainty, in the attenuation estimation is reduced by increasing N as well as by increasing the product $\sqrt{n}Z$. Since n is proportional to Z, eqn (16) shows that this uncertainty is inversely proportional to the $\frac{3}{2}$ power of Z. Thus, a longer interval, Z, will have a more significant effect in reducing the uncertainty than increasing the number of data lines, N, as has been noted by previous workers (Parker 1986; He and Greenleaf 1986; Ophir et al. 1985).

Backscatter coefficient

We had defined $RB(\omega_1)$ as the ratio of the backscatter coefficient in the sample to that in the reference phantom. A quantity $rb(\omega_1, z)$, an "estimator" of $RB(\omega_1)$ at depth z, can be computed using

$$rb(\omega_1, z) = RI(\omega_1, z)e^{4\Delta\alpha(\omega_1)z}. \quad (17)$$

This quantity is evaluated at each depth after the attenuation has been measured. Notice $rb(\omega_1, z)$ is just the ratio $RI(\omega_1, z)$, compensated by the computed attenuation. The deviation of the backscatter ratio estimator is calculated using

$$\begin{aligned} \mathrm{d}(rb) &= \frac{\partial(rb)}{\partial(RI)}\mathrm{d}(RI) + \frac{\partial(rb)}{\partial(\alpha)}\mathrm{d}(\alpha) \\ &= e^{4\alpha(\omega)z}\,\mathrm{d}(RI) + RI\cdot e^{4\alpha(\omega)z}4z\,\mathrm{d}(\alpha). \end{aligned} \quad (18)$$

Thus,

$$\frac{\mathrm{d}(rb)}{rb} = \frac{\mathrm{d}(RI)}{RI} + 4z\,\mathrm{d}(\alpha). \quad (19)$$

The standard deviation of $rb(\omega_1, z)$, $\sigma_{rb}(\omega_1, z)$, should therefore, satisfy the equation

$$\begin{aligned} \left(\frac{\sigma_{rb}}{rb}\right)^2 &= \left(\frac{\sigma_{RI}}{RI}\right)^2 + (4z\sigma_\alpha)^2 \\ &= \frac{k^2(N+N')}{NN'} + \frac{12k^2z^2(N+N')}{nZ^2NN'}. \end{aligned} \quad (20)$$

In our applications, the backscatter ratio $RB(\omega_1)$ is estimated by averaging $rb(\omega_1, z)$ over a depth interval assumed to have the same acoustic properties. If there are n independent data points within this interval (*i.e.*, the same interval is used for the backscatter coefficient as for the attenuation coefficient), then

$$\left(\frac{\sigma_{RB}}{RB}\right)^2 = \frac{k^2(N+N')}{nNN'} + \frac{12k^2\overline{z^2}(N+N')}{nZ^2NN'} \quad (21)$$

where $\overline{z^2}$ is the mean square depth and $\sigma_{RB}(\omega_1, z)$ is the standard deviation of $RB(\omega_1)$. If the depth interval is from $z_0 - Z/2$ to $z_0 + Z/2$, the mean square depth is estimated using

$$\overline{z^2} \approx \frac{1}{Z}\int_{z_0-Z/2}^{z_0+Z/2} z^2\,\mathrm{d}z = z_0^2 + \frac{Z^2}{12}. \quad (22)$$

As eqn (21) shows, the statistical uncertainty of the backscatter coefficient ratio has two sources. One is the statistical uncertainty in the $RI(\omega_1, z)$ itself, which is random and depends on the number of independent acoustic lines as well as the number of independent samples along each line. The other is propagated from the statistical error in the attenuation estimation, which introduces a dependence on z_0, the center depth of the region considered as well as on Z, the length of the depth interval over which data are averaged.

EXPERIMENTAL METHODS

As an example of the use of eqns (16) and (21), echo signal data recorded from a test phantom were analyzed to measure statistical uncertainties in the attenuation and backscatter coefficients. The properties of the test phantom, as well as those of the reference phantom are shown in Table 1. Both the reference and the test phantoms are right circular cylinders 10 cm in diameter and 6 cm thick. Each side has 50 μm Saran layers that serve as acoustic windows. The tissue mimicking material consists of water-based gel with glass bead scatterers. The diameter distribution of the beads is sharply peaked at 88 μm and is the same for both phantoms. Since the glass bead concentration is also the same (6.0 g/L, the density is 2.38 g/cm^3), both phantoms have the same expected backscatter coefficient. The phantoms differ in their attenuation coefficients, the test phantom exhibiting soft tissue-like attenuation, obtained by adding graphite power (50.0 g/L) to the gel in its molten state. The reference phantom has relatively low attenuation due mainly to absorption by the gel. Both the speed of sound and the attenuation coefficient of the phantom material were measured independently using a narrow band substitution technique (Madsen et al. 1978). Attenuation vs. frequency data were fit to a function of the form $\alpha(f) = \alpha_1 f + \alpha_2 f^2$, where f is the frequency in MHz. The constants α_1 and α_2 are presented in Table 1 for both phantoms.

The experimental set up for recording echo signals is shown in Fig. 3, and is similar to that described in a previous paper (Yao et al. 1990a). A Siemens Sonoline SL-1 scanner was used with a 5 MHz, 14 mm diameter single element transducer (KB-AEROTECH DELTA 5.0 MHz/.50, PN 2800-1, D20990) to acquire echo signals. Radio frequency echo signals were acquired after time-gain-compensation (TGC) but before envelope detection. Signals were digitized in a Lecroy TR8828C high-speed transient recorder with 8 bit precision at a rate of 50 M samples/s. Twenty separate data sets were recorded from both the reference and the sample using the same transducer and receiver gain setting. Each set consisted of echo signals along 50 independent acoustic lines, obtained by positioning the transducer at different locations on the sample window. A burst control circuit

Table 1. Properties of the phantoms.

Phantom	Attenuation α_1 dB/cm/MHz	Attenuation α_2 dB/cm/MHz^2	Speed of sound m/s	Density g/cm^3	Scatterer diameter μm
Reference	0.14050	0.0252	1587	1.02	88.6
Test	0.44420	0.0198	1580	1.05	88.6

($\alpha = \alpha_1 f + \alpha_2 f^2$ dB/cm; f is the frequency in MHz.)

designed and constructed in our laboratory (Boote et al. 1988) is used to control the timing and activate the transient recorder only when data from the region of interest is present. For both phantoms, signals were recorded from a depth interval of 0.7–5.3 cm below the scanning window.

Signal processing was done off-line in a manner described previously (Yao et al. 1990a). Quadrature detection is used to obtain the squared-amplitude data. Echo signals are fed into two parallel channels where they are multiplied by orthogonal sinusoidal waves at the analysis frequency and low-pass filtered. Signals from the two channels are the real and the imaginary parts of the filtered signal; they are then squared and combined, forming the squared-amplitude data. The analysis frequency can be changed by changing the frequency of the orthogonal sinusoidal waves. The time window used is a 3-term Blackman–Harris window whose duration is 4 μs.

Axial measurements were taken every 0.64 μs, corresponding to a depth increment of 0.5 mm. Thus the $i(\omega_1, z)$ data are correlated in the axial direction. An autocorrelation analysis of the squared-amplitude data was conducted to calculate n, the number of effective independent measurements in a depth range. Correlation coefficients between axial data points were computed at each depth and each frequency analyzed. Since most of the axial correlation is introduced by the 4 μs time window, the correlation calculation did not exhibit a strong depth or frequency dependence. If there are m measurements of $i(\omega_1, z)$ within any depth interval, the number of effective independent measurements was computed using

$$n = \frac{m^2}{m + 2\sum_{j=1}^{m-1}(m-j)\mathrm{cor}(j)} \tag{23}$$

where cor(j) is the average correlation coefficient between measurements that are j depth increments apart. The derivation of this equation and the details of the autocorrelation analysis have been described elsewhere (Yao 1990b). For this experiment, eqn (23) yielded 6.8 effective independent measurements per cm (per 13 μs).

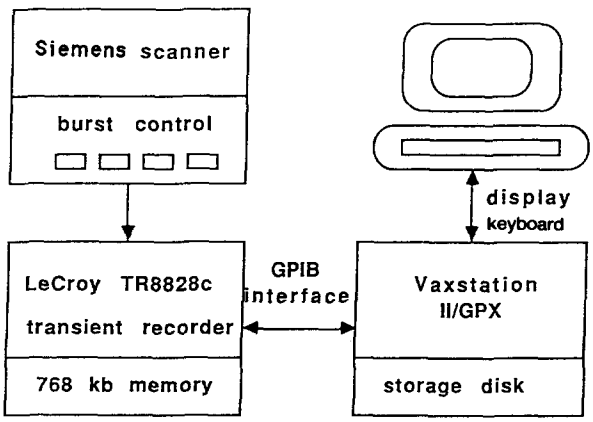

Fig. 3. Setup for digitizing radio-frequency echo signal waveforms from a clinical scanner.

RESULTS

Both the reference phantom and the sample have about 6.9 scatters/mm^3. Since the resolution element of the transducer is on the order of several cubic millimeters, there are many scatterers within one resolution element and Rayleigh statistics are expected to apply (Wagner et al. 1983). For each set of data, the average and the standard deviation of the squared-amplitude, $i(\omega, z)$, were computed as a function of depth for frequencies throughout the bandwidth of the transducer. Signal-to-noise ratios for the squared-amplitude data from both the reference and the test phantom are shown in Table 2 for three different frequencies. These ratios are nearly 1, verifying that Rayleigh statistics apply. Therefore, in subsequent computations, we have used $SNR_0 = 1$ or $k = 1$.

Fig. 4 presents results of an intermediate step in processing the data to estimate the attenuation and backscatter coefficients of the test phantom. Shown are the $RI(\omega_1, z)$ ratios, plotted as a function of depth for a set of data from 50 acoustic lines. Ratios at 3 different frequencies, indicated in the lower left of the diagram, are presented. The error bar in the top right

Table 2. *SNR* of squared amplitude.

Frequency (MHz)	Phantom	
	Reference	Test
4.25	0.997	1.013
5.0	1.017	0.998
5.75	0.969	0.998

of this figure is the computed standard deviation of the $RI(\omega_1, z)$ ratios.

Measurement results of $\Delta\alpha$, the difference between the attenuation coefficients of the test sample and the reference phantom, are presented in Table 3 for seven different frequencies. Column 2 in this table lists the attenuation coefficient differences obtained from substitution measurements (Madsen et al. 1978), and column 3 lists those computed using scattered echo signals and the reference phantom method (RPM). A similar analysis was carried out for all 20 sets of data, and standard deviations of the results are shown in column 4 of this table. The expected standard deviation was computed using eqn (14), with N and N' both 50 and $n = 27.2$ (6.8 independent samples per cm, 4 cm range). The result is 0.072 dB/cm, in reasonable agreement with the standard deviations reported in column 4.

When data from a smaller (or larger) depth interval are used to estimate the attenuation coefficient, both n and Z (eqn 14) affect the statistical error.

Table 3. Attenuation coefficient difference of the test phantom and the reference phantom. Results are shown both for through transmission, substitution measurements and for the reference phantom method (RPM).

Frequency (MHz)	Substitution	RPM (50 lines, 4 cm range)	
	Attenuation difference (dB/cm)	Attenuation difference (dB/cm)	Standard deviation (dB/cm)
4.25	1.193	1.291	0.0709
4.50	1.257	1.355	0.0926
4.75	1.321	1.431	0.0776
5.00	1.384	1.506	0.0686
5.25	1.446	1.581	0.0538
5.50	1.507	1.656	0.0613
5.75	1.568	1.732	0.0685

Table 4 presents similar data as shown in Table 3, only the depth interval is halved. The expected standard deviation is 0.204 dB/cm, computed using $Z = 2$ cm, $n = 13.6$ and N and N' the same as the previous case. The results in column 3 of this table are again in reasonable agreement with the expected value.

Measured ratios of the backscatter coefficient in the test sample to that in the reference phantom are presented in Table 5 for 7 frequencies. Also shown are the standard deviation and percentage standard deviation computed from the experimental data. No-

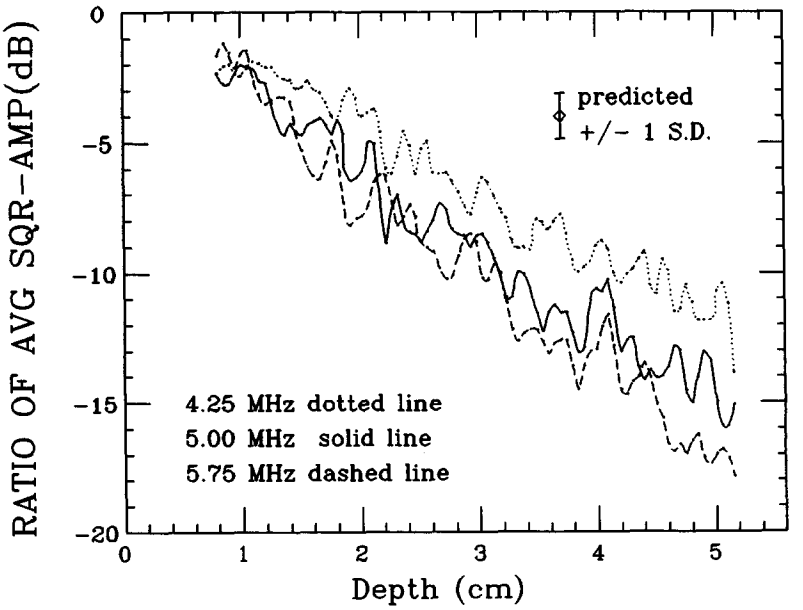

Fig. 4. The ratio of the average squared-amplitude from the sample to that from the reference phantom vs. depth. This ratio is free of depth-dependent instrumentation factors. From the slope, the attenuation coefficient difference for the two phantoms can be estimated. The curves here are ratios of data averaged from 50 independent lines. The predicted standard deviation of the ratio is ± 0.866 dB in this case.

Table 4. Attenuation coefficient difference between the test and reference phantoms for a 2-cm depth interval.

Frequency (MHz)	Attenuation (dB/cm)	Standard deviation (dB/cm)
4.25	1.278	0.2078
4.50	1.306	0.2075
4.75	1.429	0.1570
5.00	1.615	0.1638
5.25	1.731	0.1972
5.50	1.764	0.2396
5.75	1.781	0.1937

Table 5. Measured backscatter coefficient ratios for the test phantom and the reference phantom (50 lines, depth from 1 to 5 cm).

Frequency (MHz)	BSC ratio	Standard deviation	% error
4.25	1.039	0.1015	9.77
4.50	1.096	0.1154	10.53
4.75	1.136	0.1325	11.66
5.00	1.101	0.1491	13.54
5.25	1.057	0.1306	12.36
5.50	1.044	0.1161	11.12
5.75	1.060	0.0889	8.39

tice in column 2, the backscatter coefficient ratio is nearly 1 at all frequencies. As mentioned previously, the phantoms have identical glass bead scatterers with the same number per unit volume, so the expected backscatter ratio is 1. The standard deviation of the backscatter coefficient ratio is expected to be 11.3% using eqn (21). Except for the extrema in the frequencies analyzed, measured results for the 20 data set yielded a percent standard deviation close to this value.

Figure 5 illustrates expected and actual increases in the percent standard deviation when the depth interval Z (over which the backscatter ratios are averaged) is shortened. The lower set of data in this figure presents the percent standard deviation when the depth interval over which the backscatter coefficient ratio is computed is 1–5 cm. The solid line is the expected percent standard deviation. The middle set of data reports experimental and expected percent standard deviations when the depth interval 1–3 cm is used. The upper data set corresponds to the interval 3–5 cm, illustrating a further increase in the statistical uncertainty when data are obtained from deeper into the phantom. The experimental standard deviations, computed for all 20 data sets, are in reasonable agreement with the expected uncertainty (solid line) in each case.

DISCUSSION

The expressions deduced for estimating statistical uncertainties in backscatter and attenuation coefficients predicted standard deviations of these quantities reasonably well. The error in the attenuation and the backscatter coefficient increases as the depth interval, Z, over which parameters are computed is

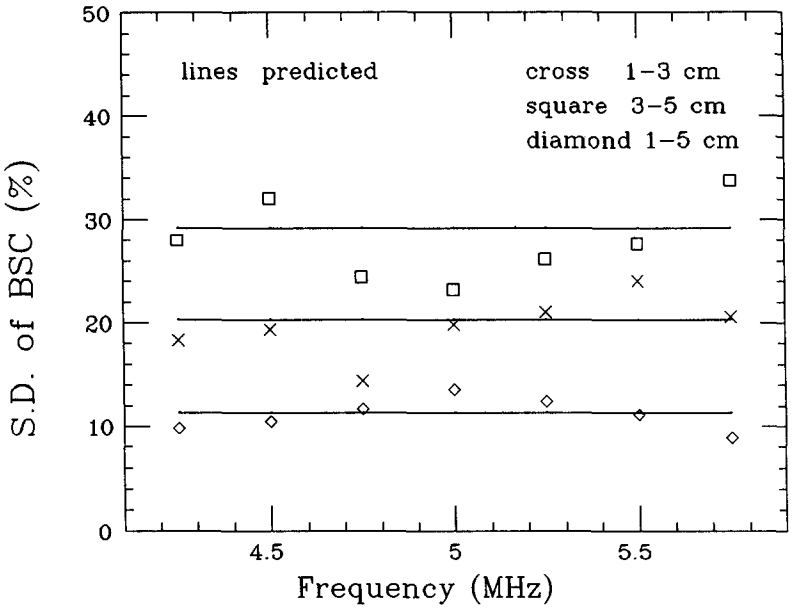

Fig. 5. Uncertainty in backscatter coefficient computations. The experimental results (data points) are compared with theoretical predictions (lines). As predicted, the 4-cm depth interval set (diamonds) is less uncertain than the 2-cm interval sets. For the 2-cm sets, the deeper one (squares) has more statistical fluctuations than the shallow one (crosses).

shortened. In the case of the backscatter coefficient, the error also increases when the distance to the region of interest is increased because of the dependence of backscatter measurements on the overlying attenuation. For *in vitro* backscatter measurements, however, this error is often minimized using a separate, through transmission measurement of the attenuation coefficient (Hall et al. 1989).

We only considered statistical uncertainties in this study. Naturally, systematic errors as outlined in the introduction also must be considered in making a final estimate of backscatter and attenuation coefficient uncertainties. These usually can be minimized by careful calibrations of the measurement system and by understanding the properties of the medium. However, the statistically based error, depending mainly on the size of the volume interrogated, which limits N, the number of data lines and Z, the depth interval over which properties can be assumed to be constant, will remain.

Acknowledgment—This work was supported in part by Grants RO1-CA25634 and RO1-CA39224 from the National Institutes of Health, and by Radiation Measurements, Inc.

REFERENCES

Bevington, P. B. Data reduction and error analysis for physical sciences. New York: McGraw-Hill; 1969:117.

Boote, E. J.; Zagzebski, J. A.; Madsen, E. L.; Hall, T. J. Instrument independent acoustic backscatter coefficient imaging. Ultrasonic Imaging 10:121–138; 1988.

Hall, T. J.; Madsen, E. L.; Zagzebski, J. A.; Boote, E. J. Accurate depth-independent determination of acoustic backscatter coefficients with focused transducers. J. Acoust. Soc. Am. 85:2410–2416; 1989.

He, P.; Greenleaf, J. F. Attenuation estimation of phantoms—A stability test. Ultrasonic Imaging 8:1–10; 1986.

Kuc, R. Bounds on estimating the acoustic attenuation of small tissue regions from reflected ultrasound. Proceeding of the IEEE 73:1159–1168; 1985.

Madsen, E. L.; Zagzebski, J. A.; Banjavic, R.; Jutila, R. Tissue-mimicking materials for ultrasound phantoms. Med. Phys. 5:391–394; 1978.

Ophir, J.; Mcwhirt, R.; Maklad, N.; Jaeger, P. A narrowband pulse-echo technique for *in vivo* ultrasonic attenuation estimation. IEEE Trans. Biomed. Engr. BME-32:205–212; 1985.

Parker, K. J. Attenuation measurement uncertainty caused by speckle statistics. J. Acoust. Soc. Am. 80:727–734; 1986.

Tuthill, T. A.; Sperry, R. H.; Parker, K. J. Deviation from Rayleigh statistics in ultrasonic speckle. Ultrasound Imaging 10:81–89; 1988.

Wagner, R. F.; Smith, S. W.; Sandrick, J. M.; Lopez, H. Statistics of speckle in ultrasound B-scans. IEEE Trans. Son. Ultrason. 30:156–163; 1983.

Yao, L. X.; Zagzebski, J. A.; Madsen, E. L. Backscatter coefficient measurements using a reference phantom to extract depth-dependent instrumentation factors. Ultrasonic Imaging 12:58–70; 1990a.

Yao, L. X. Reference phantom method for acoustic backscatter coefficient and attenuation coefficient measurement. Doctoral dissertation. Chapter 8. University of Wisconsin-Madison; 1990b.